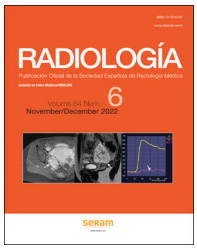
Radiología 67 (2025) 101602

RADIOLOGÍA

www.elsevier.es/rx



UPDATE IN RADIOLOGY

Ophthalmological emergencies

M.C. Maciá Fernández[a,b,*], G. Santabrígida Oreja[a], L.H. Vargas Alvarado[a], S. Sánchez Bernal[a,b], A.B. Valentín Martín[a,b], J. Encinas de la Iglesia[a]

[a] *Servicio de Radiodiagnóstico, Hospital Universitario de Salamanca, Salamanca, Spain*
[b] *Sección de Radiología de Urgencias, Hospital Universitario de Salamanca, Salamanca, Spain*

Received 25 January 2024; accepted 22 April 2024
Available online 15 September 2025

KEYWORDS
Computed tomography;
Protocol;
Ocular infection;
Retinal detachment;
Choroidal detachment;
Lens dislocation;
Eye injuries;
Intraocular foreign bodies;
Carotid cavernous fistula;
Eye inflammation

Abstract Urgent ophthalmic pathology can be grouped into four categories: infectious, traumatic, vascular, and inflammatory. Imaging techniques play a fundamental role in their diagnosis, positioning the radiologist at the forefront when dealing with these entities. CT is usually the technique of choice within the emergency context, with MRI and ultrasound playing a secondary role. Radiologists must be familiar with the main imaging findings of these pathologies to make a rapid and accurate diagnosis that contributes to a positive outcome for the patient. This article reviews orbital anatomy, imaging techniques and protocols that should be employed, as well as key diagnostic clues that every radiologist should know.
© 2024 SERAM. Published by Elsevier España, S.L.U. All rights are reserved, including those for text and data mining, AI training, and similar technologies.

PALABRAS CLAVE
Tomografía computarizada;
Protocolo;
Infección ocular;
Desprendimiento de retina;
Desprendimiento coroideo;

Urgencias oftalmológicas

Resumen La patología oftálmica urgente se puede agrupar en cuatro categorías: infecciosa, traumática, vascular e inflamatoria. Las técnicas de imagen juegan un papel fundamental en su diagnóstico, lo que posiciona al radiólogo en el primer eslabón de estas entidades. La TC suele ser la técnica de elección dentro del contexto urgente, presentando la RM y la ecografía un papel secundario. Los radiólogos debemos estar familiarizados con los principales hallazgos de imagen de estas patologías para poder realizar un diagnóstico rápido y preciso que contribuya

* Corresponding author.
E-mail address: mcmaciafernandez@gmail.com (M.C. Maciá Fernández).

2173-5107/© 2024 SERAM. Published by Elsevier España, S.L.U. All rights are reserved, including those for text and data mining, AI training, and similar technologies.

Luxación cristalino;
Daño ocular;
Cuerpos extraños intraoculares;
Fístula carótido-cavernosa;
Inflamación ocular

a la buena evolución del paciente. Este artículo repasa la anatomía orbitaria, las técnicas y protocolos de imagen que se deben emplear, así como las claves diagnósticas que todo radiólogo debe conocer.
© 2024 SERAM. Publicado por Elsevier España, S.L.U. Se reservan todos los derechos, incluidos los de minería de texto y datos, entrenamiento de IA y tecnologías similares.

Introduction

In the emergency setting, vision loss can result from infectious, traumatic, inflammatory or vascular processes.[1] Clinical assessment may be limited by several factors, such as periorbital involvement, anterior chamber injuries that hinder evaluation of posterior structures, a low level of consciousness, extensive facial trauma, or life-threatening injuries.[2] Radiologists are therefore often the first to identify ocular lesions.

Computed tomography (CT) is the imaging technique of choice due to its wide availability, speed, ability to assess the bony structures of the orbit, detect foreign bodies, and evaluate the globe and its adnexa.[1–4] Ultrasound can be useful for assessing the contents of the globe, such as hyphaema, lens dislocation or vitreous haemorrhage. However, it is operator-dependent and contraindicated when globe rupture is suspected.[1,2,4–6] Due to its superior soft tissue resolution, magnetic resonance imaging (MRI) is the preferred technique for evaluating the soft tissues and visual pathways. It is typically less available in the emergency setting and is contraindicated when the presence of foreign bodies is suspected, particularly if they are thought to be ferromagnetic.[1–4]

We will review the most common pathologies within these four categories, including an anatomical overview, a proposed CT protocol for the assessment of orbital disease, and a brief explanation of the most common mimics of emergency ophthalmological conditions.

Anatomical overview and normal CT imaging findings

The globe is located in the most anterior portion of the orbit. Its wall is composed of three layers (Fig. 1)[2,5,7–10]:

- *Cornea and sclera*. Outermost layer. It is formed by the cornea in the anterior part and the sclera in the posterior part. The sclera is perforated by the optic nerve, where it fuses with its sheath, which is composed of dura mater and arachnoid.[7] It is the site of insertion of the extraocular muscles.[8,10] It is enveloped by a fascia known as Tenon's capsule.[7–9]
- *Uveal tract*. Middle layer. It is a pigmented vascular layer composed of the choroid, ciliary body and iris. The choroid extends from the optic nerve to the ora serrata, beyond which it continues as the ciliary body. The iris forms the anterior portion of the uvea.[7,10]
- *Retina*. Innermost layer. Broadly speaking, it can be described as consisting of two layers: the outer layer, attached to the choroid and known as the retinal pigment epithelium, and the inner or sensory layer, in contact with the vitreous body.[7,8,10] The sensory retina extends from the optic disc (the site where the axons of millions of retinal ganglion cells converge to form the optic nerve)[11] to immediately posterior to the ciliary body. Here, the neural tissues of the retina terminate, and its anterior margin forms a serrated ring known as the ora serrata.[7,8,10]

The lens, identified on CT as a hyperdense, oval-shaped structure,[6] divides the eye into two segments: anterior and posterior. The anterior segment contains the aqueous humour, and the iris divides it into an anterior chamber and a posterior chamber. The posterior segment contains the vitreous humour and accounts for two-thirds of the volume of the globe.[2,5–7,10]

CT does not allow differentiation of the three layers of the globe, so a single, thin, slightly hyperdense layer is seen forming the wall of the posterior region of the globe.[5,9]

There are three potential spaces within the eye that can accumulate fluid, leading to detachment of different layers of the globe: (1) the posterior hyaloid space, between the vitreous base and the sensory retina; (2) the subretinal space, between the sensory retina and the retinal pigment epithelium; and (3) the suprachoroidal space, between the choroid and the sclera. The episcleral or Tenon's space is also present, located between the outer surface of the sclera and the inner surface of Tenon's capsule.[7]

There are six *extraocular muscles*: four rectus muscles (superior, inferior, lateral and medial)[2,12] and two oblique muscles (superior and inferior).[12] Some authors consider the levator palpebrae superioris muscle to be the seventh extraocular muscle.[6,13,14]

The rectus muscles converge at the orbital apex to form the *orbital or muscular cone*, which divides the orbit into the intraconal space—located within the muscular cone—and the extraconal space—located outside it.[2]

There is a fibrous membrane known as the orbital septum (a virtual structure not identifiable on imaging), which extends from the orbital periosteum to the tarsal plate of both eyelids, separating the orbit from the external soft tissues.[1,2] It defines a *preseptal space* (anterior to the orbital

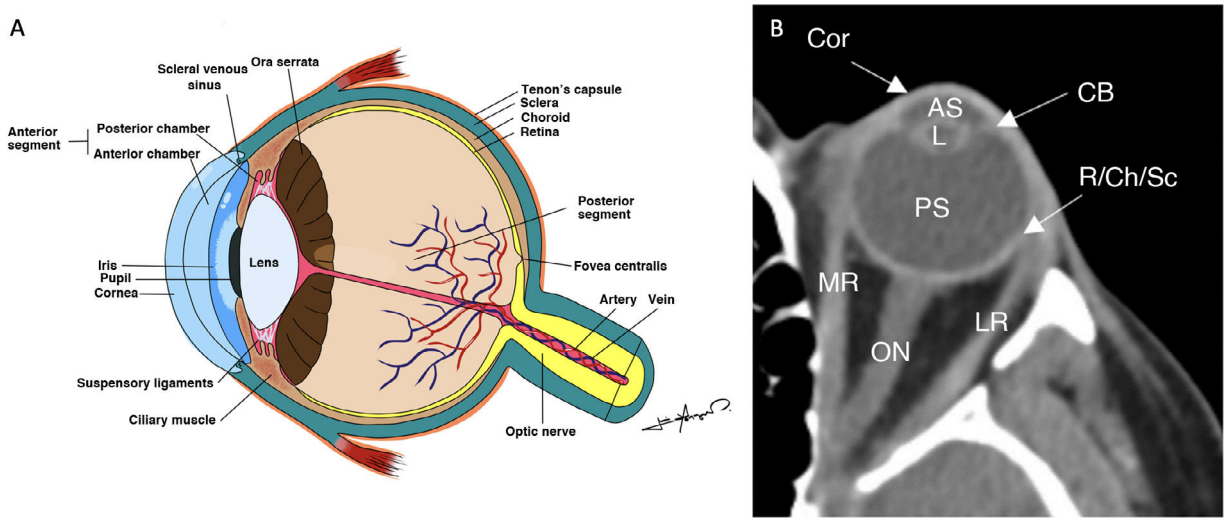


Figure 1 Anatomy of the globe. (A) Anatomical illustration of the globe. (B) Representation of globe anatomy on non-contrast orbital CT. CT does not allow differentiation of the three layers of the globe, so the retina (R), choroid (Ch), and sclera (Sc) appear as a single thin layer that is slightly hyperdense compared to the contents of the anterior (AS) and posterior (PS) segments, forming the wall of the posterior region of the globe. In the anterior part, the cornea (Cor) can be identified. The lens (L) appears as a hyperdense, oval-shaped structure that divides the globe into anterior and posterior segments, anchored to the sclera by the ciliary body (CB). The sclera is perforated posteriorly by the optic nerve (ON) and serves as the insertion site for the extraocular muscles (MR: medial rectus; LR: lateral rectus).

Table 1 Imaging protocol for the diagnosis of orbital disease using CT.

ORBITAL CT	
Acquisition	Helical, cranio-caudal. Bone and soft tissue windows
Anatomical coverage	From the roof of the frontal sinus to the hard palate.
kVp/mA range	120 kVp, 100 mAs
Slice thickness	Thin-section thickness 1.25 mm; 1.25 mm interval
Intravenous contrast	*Traumatic disease/suspected foreign body*: without intravenous contrast Suspected *infectious/inflammatory disease*: 70 ml at 2 ml/s with a 70–100 s delay Suspected *vascular lesion* (carotid–cavernous fistula, aneurysms): CT angiography from vertex to C1 using bolus tracking with ROI in the aortic arch and attenuation threshold of 80–100 HU. Administer 60–70 ml of intravenous contrast at 4–5 ml/s. An additional acquisition at 70–100 s may be included.
Post-processing	Multiplanar reconstructions in bone and soft tissue windows. Oblique coronal reconstruction perpendicular to CN II and oblique sagittal reconstruction parallel to CN II are recommended.

CN II: cranial nerve II (optic nerve); ROI: region of interest.

septum) and a *postseptal space*, or the orbit proper, and acts as a natural barrier against the spread of infection.[1,2]

CT imaging protocol

Table 1 provides a detailed summary of the CT protocol according to the reviewed literature.[2,15–17] The American College of Radiology (ACR) Appropriateness Criteria, updated in 2017,[16] recommend that when there is clinical suspicion of inflammatory, infectious, neoplastic or vascular disease, the initial examination should be a CT of the orbits performed directly after intravenous contrast administration, on the grounds that the baseline study does not provide relevant information.

Conversely, the initial evaluation of orbital trauma or a suspected foreign body should be carried out without intravenous contrast, except when associated vascular disease is suspected.[15–17]

Infectious disease

Preseptal and postseptal cellulitis

Cellulitis is an infection of the skin or soft tissues surrounding the globe. Determining whether the infection is preseptal or postseptal determines clinical management (Table 2, Fig. 2).[1,18–21]

If infection does not extend beyond the orbital septum, it is termed preseptal cellulitis or periorbital cellulitis, and

Table 2 Characteristics of preseptal (periorbital) cellulitis and postseptal (orbital) cellulitis.

	Preseptal (periorbital) cellulitis	Postseptal (orbital) cellulitis
Location	Limited to the soft tissues anterior to the orbital septum	Spread to soft tissues posterior to the orbital septum
Therapeutic management	Oral antibiotics	Hospital admission. Intravenous antibiotic therapy. Monitoring for possible complications (orbital or intracranial abscesses, meningitis, cavernous sinus thrombosis or superior ophthalmic vein thrombosis)
Causes	Contiguous spread of infection from adjacent structures: face, teeth, and ocular adnexa. Local trauma	Perivascular spread of infection from paranasal sinusitis (most frequently ethmoidal).

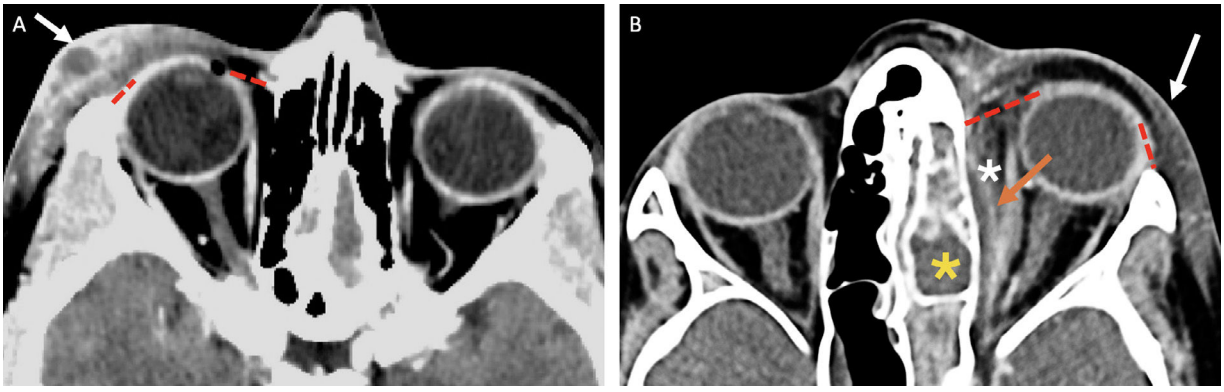


Figure 2 Orbital and periorbital cellulitis. Axial sections from contrast-enhanced orbital CT scans from two different patients, with red lines indicating the theoretical location of the orbital septum. (A) Preseptal cellulitis in a 21-year-old woman, consistent with periorbital inflammatory changes with a small abscess (white arrow). (B) Preseptal and postseptal cellulitis in a 12-year-old boy following an upper respiratory tract infection. Periorbital oedema (white arrow). Opacification of the left ethmoidal air cells (yellow asterisk) consistent with sinusitis, associated with a subperiosteal abscess (orange arrow) and inflammatory involvement of the adjacent extraconal fat (white asterisk).

is caused by contiguous spread from adjacent structures or by local trauma.

If it extends posterior to the orbital septum, it is termed *postseptal cellulitis or orbital cellulitis*, and is usually secondary to perivascular spread from a paranasal sinusitis.

Endophthalmitis/panophthalmitis

Endophthalmitis is inflammation of the deep layers of the globe, although in clinical practice the term refers to inflammation secondary to an intraocular infection.[20–22]

If the inflammation progresses to involve the sclera and subsequently Tenon's capsule, thereby affecting all layers of the globe, it is referred to as *panophthalmitis*.[22,23]

Infectious endophthalmitis may be exogenous (following ocular surgery, penetrating trauma, or spread from a contiguous infectious process) or endogenous (haematogenous dissemination from a primary infectious focus, typically in immunocompromised patients or intravenous drug users).[9,21,22,24]

Exogenous infection secondary to cataract surgery is the most common cause of the disease.[9,22] Diagnosis of endophthalmitis relies on clinical assessment. Imaging studies, particularly CT and MRI, are useful for assessing the extent of the disease, its progression, associated complications, and the response to treatment. Radiological findings depend on the evolutionary stage of the process and may be classified as early, advanced, or late stage (Figs. 3 and 4).

Infection originates in the choroid, owing to its rich vascular supply, and manifests as thickening and hyperenhancement of the uveal layer, particularly noticeable in comparison with the unaffected eye. If the infection progresses, it spreads to the retina and vitreous body, leading to increased attenuation of the vitreous humour due to the presence of purulent or proteinaceous exudate.[9,19]

In the *advanced stage* of the disease, this proteinaceous or purulent exudate accumulates in various compartments of the globe, such as the subretinal or suprachoroidal spaces, leading to detachment of these layers or even abscess formation. Severe cases may present with deformation of the globe and proptosis, and may even result in globe rupture. An increase in density within the anterior chamber should raise suspicion of hypopyon,[9,19] (pus in the anterior chamber of the eye).

In the *final stage*, *phthisis bulbi* may be observed—an atrophic and often calcified globe with complete loss of vision.[9]

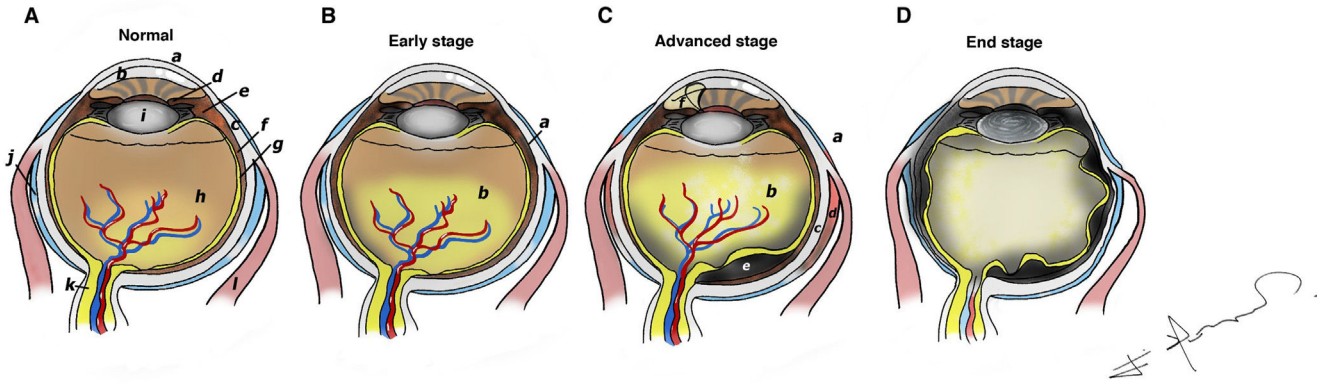


Figure 3 Illustration of normal ocular anatomy and pathophysiological progression of endophthalmitis. (A) Illustration of a healthy globe: a, cornea; b, anterior chamber; c, sclera; d, iris; e, ciliary body; f, choroid; g, retina; h, posterior segment (vitreous body); i, lens; j, Tenon's capsule; k, optic nerve; l, extraocular muscle. (B) Early stage of the disease: a, onset in the middle layer of the globe, presenting as thickening of the uveal tract; b, progression of the infection with extension into the vitreous body. (C) Advanced stage of the disease: c, spread of the infection to the sclera; d, inflammatory changes with thickening and hyperenhancement of Tenon's capsule; e, retinal detachment (exudates accumulate in the subhyaloid, subretinal or suprachoroidal spaces, leading to ocular detachments). (D) End stage of the disease, with an atrophic, disorganised globe and complete loss of vision in most cases—known as *phthisis bulbi*.

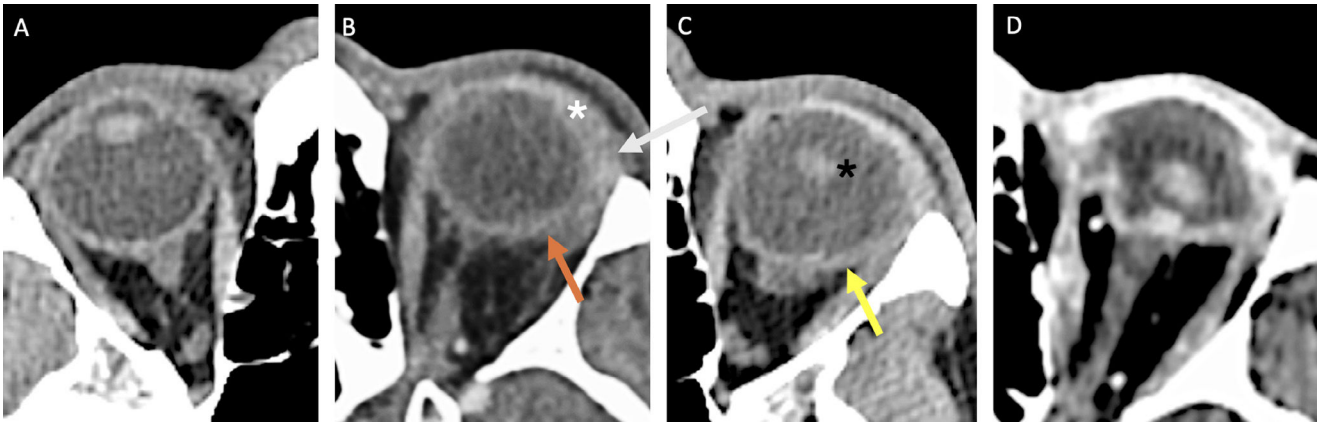


Figure 4 Unfavourable progression of endophthalmitis in left globe of a patient with diabetic retinopathy and history of vitrectomy in the left eye three weeks earlier. Axial and oblique axial sections from orbital CT scans following intravenous contrast administration. (A) Right globe with normal characteristics. (B) Early, yet progressed, stage of endophthalmitis. Smooth uveoscleral thickening and hyperenhancement (orange arrow) are observed, more evident when compared with the healthy side (A), along with episcleral inflammation corresponding to Tenon's capsule (white asterisk), which is not identifiable on CT in a healthy globe. Enlargement of the left lacrimal gland compared to contralateral side (white arrow), suggestive of secondary dacryoadenitis. These findings are indicative of panophthalmitis. (C) Advanced stage of the disease. There is distortion of the morphology and contour of the left globe, with irregular uveoscleral thickening and hyperenhancement (yellow arrow), indicating globe rupture. In addition, the lens (black asterisk) has lost its usual oval shape and is subluxated posteriorly. (D) Late stage of the disease. A disorganised globe is identified, consistent with *phthisis bulbi*, with complete loss of vision. This patient ultimately underwent enucleation of the left eye.

Traumatic disease

Orbital fractures

According to their mechanism of impact, orbital fractures are classified as *blow-out* or *blow-in* fractures. *Blow-out fractures* result from a direct impact to the orbit, causing a sudden increase in intraorbital pressure, with bony fragments displaced outward from the orbit. *Blow-in fractures* cause a reduction in intraorbital space due to the displacement of bony fragments into the orbit, which may result in proptosis.[6]

The most common type of *blow-out fracture* involves the orbital floor, with the medial wall being the next most frequently affected. Orbital floor fractures can result in herniation of intraorbital fat into the maxillary sinus and entrapment of the inferior rectus muscle, potentially causing diplopia and indicating the need for prompt surgical management (Fig. 5).[6]

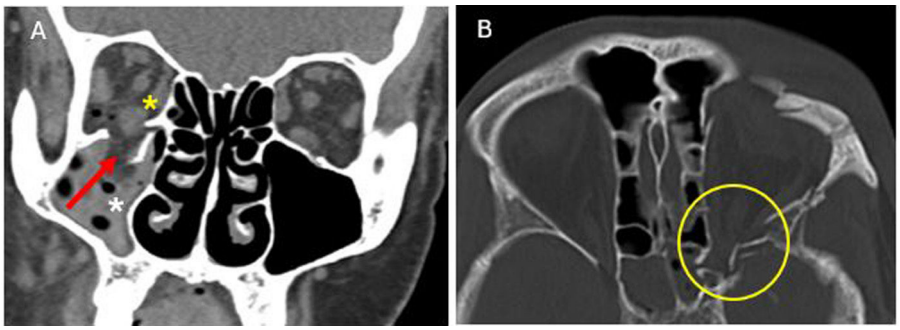


Figure 5 Orbital fractures. (A) Coronal reconstruction of non-contrast facial CT showing a fracture of the right orbital floor with herniation of periorbital fat into the maxillary sinus (red arrow). The inferior rectus muscle is enlarged and has a rounded appearance, consistent with signs of muscle entrapment (yellow asterisk). Associated blood collection in maxillary sinus (white asterisk). (B) Axial non-contrast orbital CT image using a bone reconstruction algorithm, showing a complex facial fracture involving the orbital apex with multiple bone fragments (yellow circle). Ipsilateral vision loss was confirmed as a result of optic nerve injury.

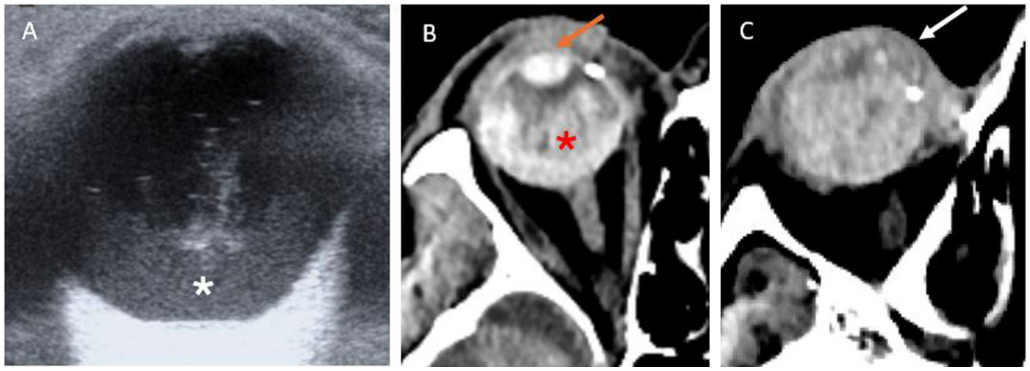


Figure 6 Traumatic disease of the globe. Hyphaema and/or vitreous haemorrhage in different patients. (A) Ocular ultrasound demonstrating echogenic material in the dependent portion of the posterior segment, consistent with vitreous haemorrhage (white asterisk). (B) Hyphaema and vitreous haemorrhage on axial non-contrast orbital CT. There is increased attenuation in the posterior segment, compatible with vitreous haemorrhage (red asterisk), and a small amount of high-density material in the anterior chamber, anterior to the lens, consistent with hyphaema (orange arrow). (C) Hyphaema and vitreous haemorrhage in woman with history of prior lens extraction. Axial non-contrast orbital CT shows an enlarged right globe with associated proptosis, with no clear distinction between the anterior and posterior segments; both contain haemorrhagic material. Irregularity in the superonasal corneoscleral region (white arrow), which on physical examination corresponded to a rupture site with extrusion of blood from the anterior chamber externally.

Orbital apex fractures, located in the posterior aspect of the orbit, are particularly important among orbital fracture types (Fig. 5). These may involve the superior orbital fissure, resulting in injury to cranial nerves III, IV, V_1, and VI, and leading to ophthalmoplegia, diplopia and ptosis. If the optic canal is involved, cranial nerve II may be damaged, resulting in loss of vision.[6]

The role of urgent surgical decompression and corticosteroid therapy remains controversial.[25]

Hyphaema/vitreous haemorrhage

Hyphaema refers to a collection of blood in the anterior chamber of the globe, resulting from disruption of blood vessels in the iris or ciliary body[5,6] (Fig. 6). On non-contrast CT, this entity appears as a hyperdense area within the anterior chamber.[2,5,26] Hyphaema is readily identifiable on clinical examination, but it hinders adequate assessment of the posterior structures by the ophthalmologist, thereby prompting the need for imaging studies.[2,6]

Vitreous haemorrhage is the presence of blood within the vitreous humour of the posterior segment, resulting from disruption of retinal blood vessels[5] (Fig. 6). It presents as a hyperdense collection in the posterior segment on non-contrast CT.[2,5,26]

It is important to emphasise that *the presence of intraocular haemorrhage in children is highly specific (*95%*) for non-accidental trauma.*[2,27] It is necessary to complement the assessment with a baseline cranial CT to detect complications such as subarachnoid haemorrhage, subdural haematomas or skull fractures.[2]

Retinal detachment and choroidal detachment

Retinal detachment occurs due to a tear between the sensory layer of the retina and the retinal pigment epithelium, allowing fluid or blood to pass from the vitreous cavity into

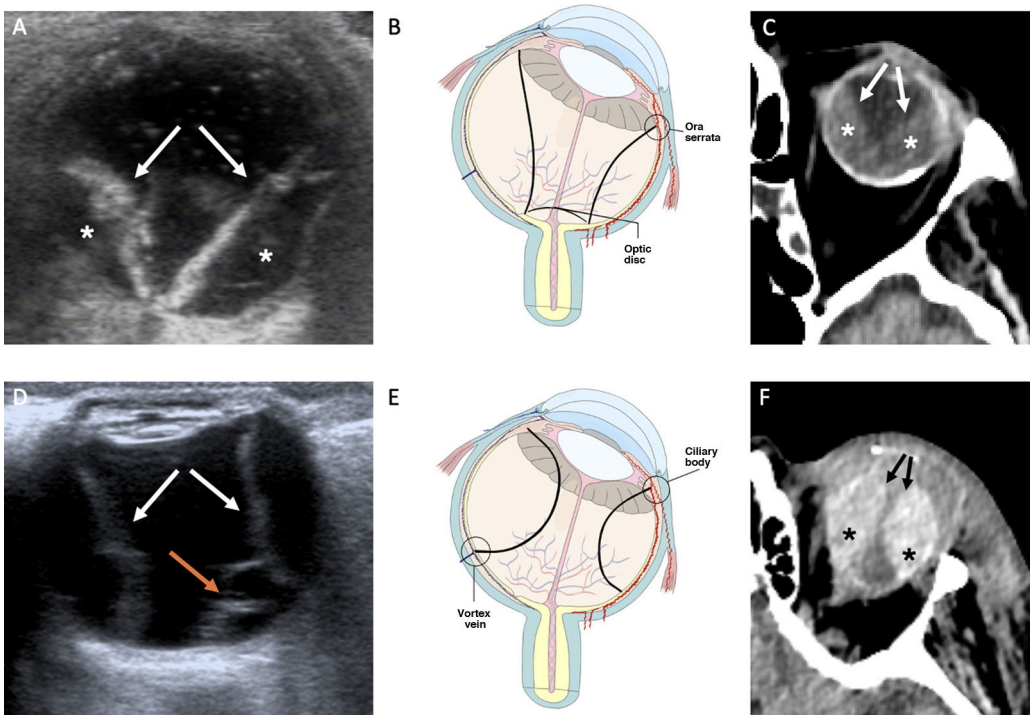


Figure 7 Retinal detachment (A, B and C) and choroidal detachment (D, E and F) across different imaging modalities. (A) Axial ocular ultrasound image. B) Illustration of the globe showing the retinal attachment sites. (C) Axial section from non-contrast orbital CT. Both in image (A) and in image (C), the characteristic 'V' shape of retinal detachment (arrows) is seen, with associated haemorrhagic component in the subretinal space (asterisks). (D) Axial ocular ultrasound image. (E) Illustration of the globe showing the choroidal attachment sites. (F) Axial section from non-contrast orbital CT. In image (D), the characteristic biconvex lens-shaped appearance of choroidal detachment (white arrows) is observed, along with an associated retinal detachment (orange arrow). In image (F), a choroidal detachment (black arrows) is seen, with blood accumulation in the suprachoroidal space (asterisks).

the subretinal space.[2,5,6,28] In the absence of suspected globe rupture, ultrasound is the imaging modality of choice for its diagnosis.[29]

On CT or ultrasound, it presents as a hyperdense or echogenic membrane representing the detached sensory retina, with subretinal fluid of either water or blood density, typically forming a *characteristic 'V' shape*. This shape is due to the firm attachment of the retina to the optic disc posteriorly and to the ora serrata anteriorly.[2,5,6] (Fig. 7)

Choroidal detachment consists of separation between the choroid and sclera due to accumulation of fluid in the suprachoroidal space, usually secondary to decreased intraocular pressure. The choroid's rich vascular supply predisposes it to vascular injury, resulting in haemorrhagic accumulation that is identified as hyperdense on CT or hyperechogenic on ultrasound within the suprachoroidal space.[6]

Choroidal detachment typically presents with a *biconvex morphology*, displacing the choroid and retina towards the centre of the globe.[2,5,6]

Unlike retinal detachment, choroidal detachment is not anteriorly limited by the ora serrata and may extend beyond it.[2,5,6,10,23] Additionally, posteriorly, choroidal detachment diverges as it approaches the optic disc,[22] with its anchoring point at the insertion of the vortex veins, where the sclera and choroid are firmly adherent.[6,10,30] (Fig. 7)

Traumatic injuries of the lens

Ocular trauma may cause partial dislocation (subluxation) or complete dislocation (luxation) of the zonular fibres that anchor the lens to the ciliary body (Fig. 8)[2,5]:

- *Lens subluxation (partial dislocation)*: the margin of the lens still secured to the ciliary body by intact zonular fibres retains normal positioning, while the portion associated with zonular fibre rupture shows abnormal angulation.[2,5]
- *Luxation (complete dislocation)*: the lens is entirely dislocated into either the anterior or posterior segment, with posterior dislocation being most common.[5,6]

Anterior lens luxation is uncommon, as its movement is restricted by the iris[4,5]; however, its diagnosis is important, as it may trigger *angle-closure glaucoma*, which constitutes a surgical emergency.[2] It presents as a slight reduction in the anteroposterior diameter of the anterior chamber, which may be difficult to distinguish from globe rupture.[2]

Rupture of the lens capsule may lead to intralenticular oedema and the development of a *traumatic cataract*. On CT, it appears as a lens that is hypodense compared to the unaffected side (Fig. 8),[5,25] in contrast to the hyperdense or even calcified appearance of a mature cataract.[5]

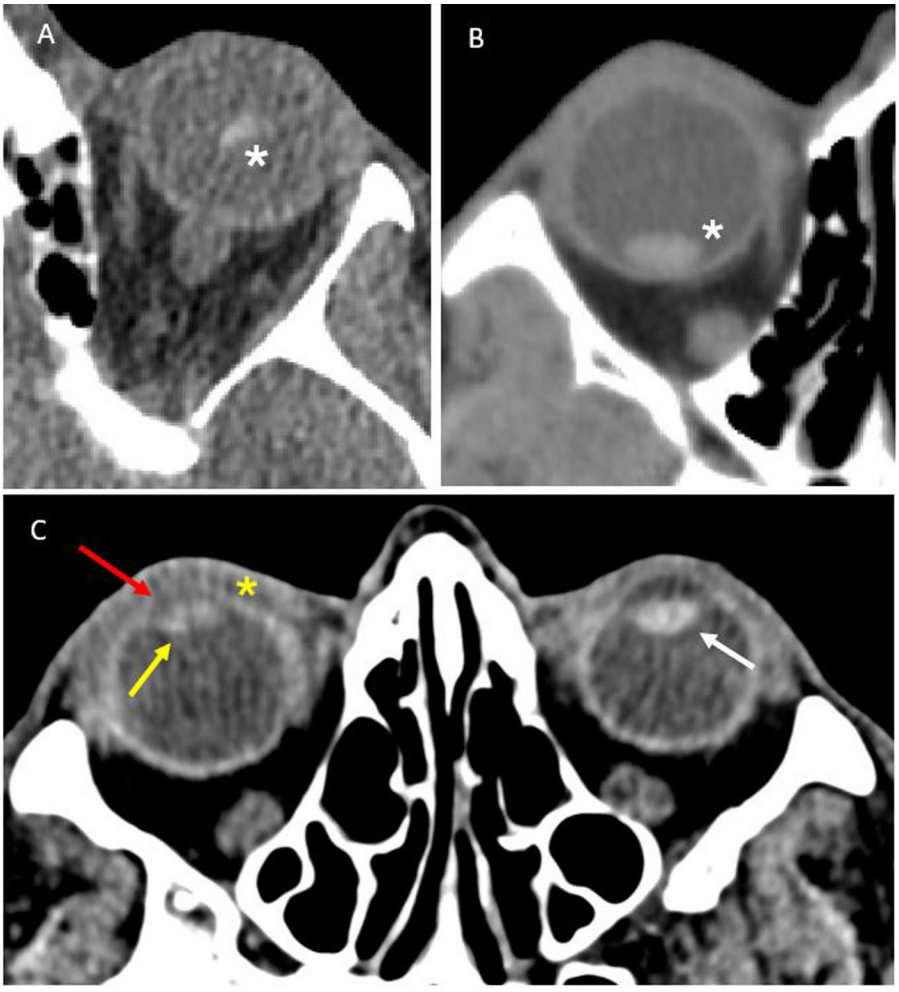


Figure 8 Lens trauma. Axial sections from non-contrast orbital CT scans. (A) Posterior subluxation (partial dislocation) of the lens. (B) Posterior luxation (complete dislocation) of the lens. (C) Traumatic cataract. The lens of the right globe (yellow arrow) appears hypodense in relation to the contralateral side (white arrow), which, in a traumatic context, is suggestive of a traumatic cataract. Reduction in the anteroposterior diameter of the anterior chamber (red arrow) compared with the left eye, compatible with corneal laceration, with a small preseptal haematoma (yellow asterisk).

Globe rupture

Globe rupture may result from either blunt or penetrating injury.[6] There are both direct and indirect signs that should raise suspicion of globe rupture[5] (Fig. 9).

Indirect signs are:

- The presence of intraocular air bubbles or foreign bodies (suggesting a breach through the sclera).[5,31]
- An altered anteroposterior diameter of the anterior chamber, increasing in posterior injuries and decreasing with corneal laceration.[5,6,31–33]

Direct signs are:

- Changes in the shape or volume of the globe.[5,6,31]
- Scleral discontinuity.[5,6]

Scleral tears typically occur near the insertions of the extraocular muscles, where the sclera is thinner.[2,5,6]

Intraocular foreign bodies

CT is the imaging modality of choice when intraocular foreign bodies are suspected, with a sensitivity that can reach up to 100%.[5]

Ultrasound may be useful for detecting foreign bodies, although it is less sensitive than CT. It is contraindicated if globe rupture is suspected.[5] Intraocular foreign bodies appear as hyperechoic foci with variable posterior acoustic shadowing, depending on their composition. Intraocular gas introduced during trauma may mimic a foreign body due to its hyperechoic appearance.[34]

Inorganic foreign bodies are the most common and primarily include metal (Fig. 9B) and glass, the latter showing variable density on CT, ranging from 80 to 550 Hounsfield units (HU)[35] (Fig. 10A). They are typically associated with vision loss and, due to their inert nature, do not usually provoke an inflammatory or infectious response.[5]

Organic foreign bodies may provoke a marked inflammatory response and carry a high risk of endophthalmitis.

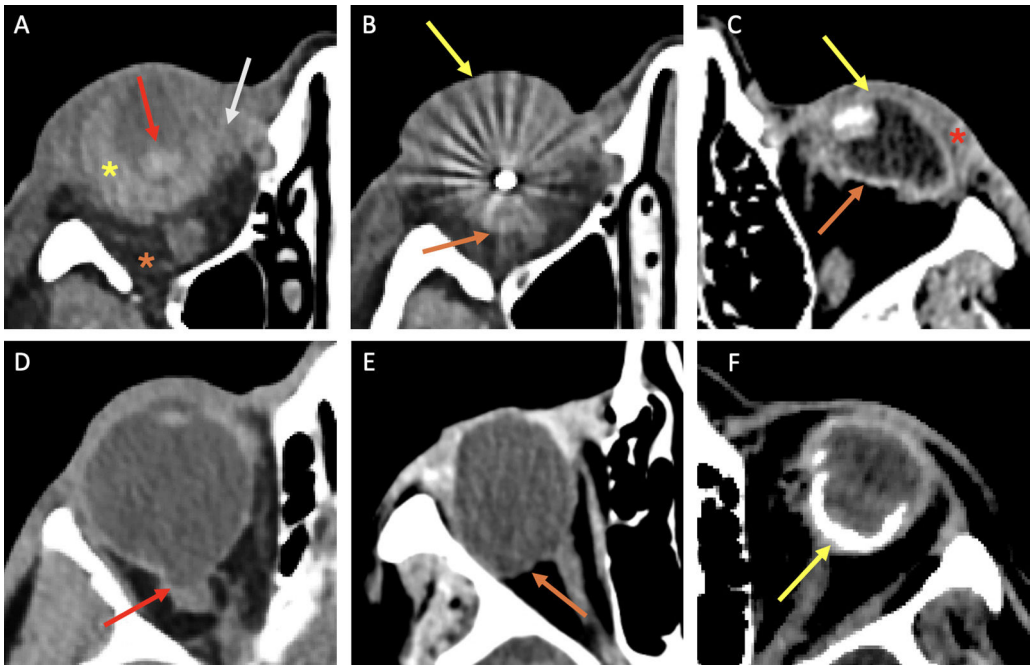


Figure 9 Globe rupture (A–C) and potential pitfalls (D–F). Axial sections from non-contrast orbital CT scans from different patients. (A and B) Rupture of the right globe due to perforation secondary to a high-density foreign body (metal) located in the posterior segment of the right eye (B), with contour irregularity of the posterior segment of the globe (orange arrow), signs of vitreous haemorrhage (yellow asterisk), and probable haemorrhagic component in the episcleral space (white arrow). Posterior luxation of the lens (red arrow), preseptal haematoma (yellow arrow), and stranding of postseptal fat (orange asterisk). (C) Signs of rupture of the left globe following blunt trauma. There is marked reduction in both the anteroposterior diameter of the anterior chamber (yellow arrow) and the posterior segment, with significant contour irregularity in the latter (orange arrow). Findings consistent with globe rupture involving both the anterior chamber and the posterior segment. There is also anterior subluxation of the lens, accompanied by a small preseptal haematoma (red asterisk).
(D) Sixteen-year-old patient with a diagnosis of right posterior coloboma. A defect is seen in the posterior segment of the globe at the site of optic nerve insertion (red arrow). (E) Increased anteroposterior diameter of the right globe with a focal prominence at the temporal margin of the posterior segment (orange arrow), indicative of posterior staphyloma in a patient with high myopia. (F) Left *phthisis bulbi* secondary to retinal detachment. A small left globe is identified, with coarse calcification outlining the contour of the posterior segment.

Wood, the most common material (Fig. 10B), may be mistaken for air on CT due to the density it initially exhibits, ranging between −100 and −200 HU. Its attenuation increases over time due to fluid accumulation. Air, however, measures approximately −1,000 HU.[2,25]

Certain patterns of intraocular calcification may mimic the appearance of radiopaque foreign bodies. Calcifications occurring near the optic disc are known as drusen and are associated with macular degeneration (Fig. 10C). Calcifications along the insertions of the medial and lateral rectus muscles are known as scleral plaques and are common in elderly patients[5] (Fig. 10D). *Phthisis bulbi*, which may result from infection, inflammation or trauma, is another potential source of diagnostic confusion (Fig. 9F).[1]

Pitfalls in the diagnosis of globe rupture

Certain postoperative findings may be misleading in the context of trauma and should be distinguished from globe rupture[6] (Fig. 11):

- *Scleral buckling*. Involves suturing a silicone material to the sclera, thereby bringing the choroid and sclera closer to the retina and reducing traction on it.[36,37] Solid silicone bands can be used, which typically exhibit values between 150 and 300 HU, or silicone sponges containing air, which generally range from −250 to −400 HU.[38]
- *Pneumatic retinopexy*. A procedure in which an intravitreal gas bubble is injected and expands to cover the retinal tear, creating a seal that prevents fluid from passing from the vitreous cavity into the subretinal space.[39,40] The gas commonly used is perfluoropropane, which exhibits the same attenuation as air on CT and may therefore be misinterpreted as a penetrating injury.[39]
- *Vitrectomy*. Involves the removal of the vitreous humour with the aim of bringing the retina closer to the choroid and sclera, using an intraocular tamponade agent—either gas or liquid, most commonly silicone oil—to seal the tear.[37–40] The resorption time of air bubbles depends on the type of gas or gas mixtures used and can range from 3 to 5 days to 2–3 months.[41] Silicone oil is permanent (unless surgically removed) and appears on CT as a high-density material within the vitreous cavity,[37] potentially mimick-

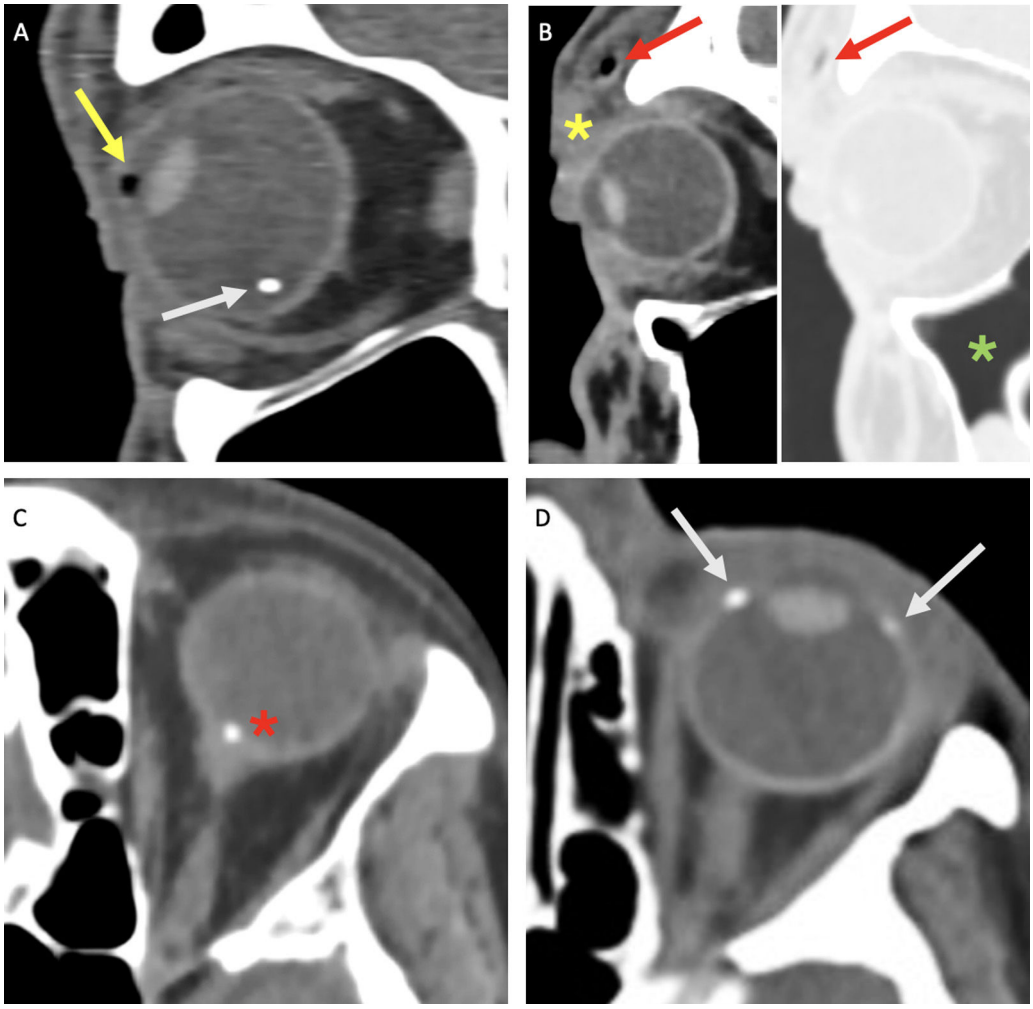


Figure 10 Foreign bodies and their mimics. Non-contrast orbital CT scans from different patients. (A) Patient with trauma to the right eye caused by a gas pressure gauge. Oblique sagittal reconstruction of the right globe showing a gas bubble in the anterior chamber (yellow arrow) and a hyperdense foreign body in the dependent portion of the posterior segment (white arrow) with a densitometric value of 557 HU, consistent with glass. (B) Patient presenting to the emergency department with whitish discharge, right eye redness, and periorbital pain following trauma while cutting pine branches. Oblique sagittal reconstruction of the right globe in soft tissue and lung windows showing a large periorbital haematoma (yellow asterisk) and a hypodense area with an attenuation value of −196 HU in the supraciliary region, consistent with a wooden foreign body. Note the higher attenuation compared with the air in the maxillary sinus (green asterisk). (C) Axial section of left globe showing punctate calcification (red asterisk) at the optic disc, consistent with drusen. (D) Axial image of the left globe showing two punctate calcifications, one at the insertion of the medial rectus muscle and the other at the insertion of the lateral rectus muscle, indicative of scleral plaques (white arrows).

ing a vitreous haemorrhage. However, silicone oil exhibits higher densitometric values than blood (100–140 HU),[38] and on MRI it shows decreased signal intensity on fat-suppressed sequences.[37,38]

There are *globe deformities* that may mimic rupture in a traumatic context (Fig. 9D and E). Congenital deformities of the globe, such as coloboma, can be encountered. This condition results in a focal defect in any of the ocular structures. On imaging studies, the affected globe is usually small, with a focal defect and herniation of the vitreous at the site of the coloboma. When located in the posterior segment, there is often widening of the optic disc, which is commonly associated with a retrobulbar cyst. If chronic, it may be associated with calcifications. Among acquired deformities, staphyloma is notable; it involves thinning of the uveal tract and sclera without an actual defect. Imaging studies reveal enlargement of the affected globe with a focal bulge, typically located at the temporal margin of the posterior segment. It is important to distinguish these entities from the typical elongation seen in a myopic eye, where no focal bulging is observed.[42]

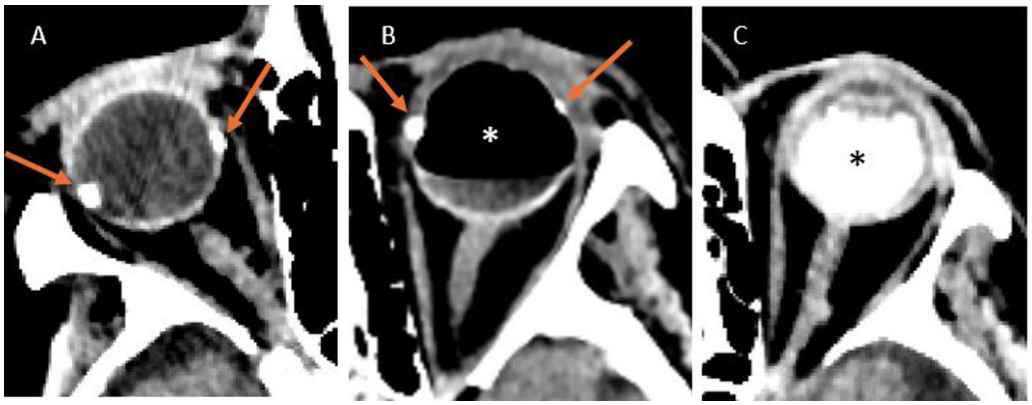


Figure 11 Techniques used in retinal detachment. Axial sections from non-contrast orbital CT scans from different patients. (A) Scleral buckling with solid silicone bands (orange arrows). (B) Combined treatment of scleral buckling using solid silicone bands (orange arrows) and pneumatic retinopexy (white asterisk). (C) Vitrectomy using silicone oil as a tamponade agent (black asterisk).

Vascular disease

Carotid–cavernous fistula

A carotid-cavernous fistula consists of an abnormal communication between the carotid circulation and the cavernous sinus.[2] The anatomical classification is the most commonly used (Table 3).[43,44] According to this classification, fistulas can be either direct or indirect, with the former being more common.[45]

The diagnosis is suggested by the presence of post-traumatic diplopia associated with proptosis, chemosis, pulsatile tinnitus or cranial nerve palsies (III, IV, V1, V2, and VI).[2,43,45,46]

Although invasive angiography is the diagnostic technique of choice,[43–45] CT provides substantial information in an emergency setting, with the following findings typically observed:

- *Signs of orbital congestion*, with proptosis, retrobulbar oedema and thickening of the extraocular muscles.[2,44]
- *Early venous dilatation and enhancement of the cavernous sinus*. In direct fistulas, due to their high-flow nature, there will be dilatation of the cavernous sinus with early enhancement showing attenuation values similar to those of the internal carotid artery in the arterial phase. However, in indirect fistulas, enhancement of the venous sinus—although showing higher attenuation values than the other sinuses in the arterial phase—does not reach those of the internal carotid artery. Therefore, performing both arterial and venous phase imaging can help differentiate a direct fistula from an indirect one. This increase in pressure will lead to a reversal of flow from the cavernous sinus, resulting in dilatation of the superior ophthalmic vein, the pterygoid venous plexuses and the ipsilateral facial vein.[25] (Fig. 12A and B).
- *Fistulous tract* from the internal carotid artery to the cavernous sinus.[46]
- *Intracranial haemorrhage* due to rupture of ectatic veins.[44]

Superior ophthalmic vein thrombosis

The most common cause of superior ophthalmic vein thrombosisis is orbital infection secondary to paranasal sinusitis.[2,47] Contrast-enhanced CT and MRI demonstrate filling defects in the superior ophthalmic vein, typically accompanied by enlargement of both superior ophthalmic veins and the cavernous sinus, as well as proptosis and orbital and periorbital oedema (Fig. 12C). Serious complications of superior ophthalmic vein thrombosis include vision loss, cavernous sinus thrombosis and sepsis if it is secondary to an infectious process.[1]

Papilloedema

The term *papilloedema* refers to optic disc oedema (usually bilateral) secondary to intracranial hypertension.[2,48] CT or MRI findings include intraocular protrusion of the optic nerve heads, flattening of the posterior aspect of the sclera, thickening of the optic nerve sheaths and bilateral tortuosity of the optic nerves. In addition, they allow the exclusion of causes of intracranial hypertension, such as space-occupying lesions, obstructive hydrocephalus or venous thrombosis.[49,50] (Fig. 13).

Inflammatory disease

Thyroid eye disease

Thyroid eye disease is the leading cause of exophthalmos in adults and is usually secondary to Graves' disease.[1] Clinical findings include eyelid retraction, proptosis, ophthalmoplegia, conjunctivitis and chemosis.[51] Classical imaging findings include symmetrical and bilateral (less commonly unilateral) thickening of the bellies of the extraocular muscles, with *sparing of their tendinous insertions* on the globe.[52] (Fig. 14) The order of involvement is as follows: inferior rectus, medial rectus, superior rectus, and lateral rectus.[1,51] Additionally, there may be an increase in orbital fat, enlargement

Table 3 Anatomical classification of carotid–cavernous fistulas and their pathophysiological classification based on angiographic findings (Barrow classification) and their causes.

Anatomical classification	• Direct (70–75%)	• Indirect (25–30%)
Barrow classification (pathophysiological)	• *Barrow type A:* direct communication between ICA and CS	• *Barrow type B:* communication between meningeal branches of the ICA and the CS • *Barrow type C:* communication between meningeal branches of the ECA and the CS • *Barrow type D:* communication between meningeal branches of the ICA and ECA
Causes	• Post-traumatic (including iatrogenic causes such as surgery, angiography) • Rupture of an aneurysm of the cavernous segment of the ICA • Vasculopathies: collagen deficiency syndrome, fibromuscular dysplasia, etc.	• CS thrombosis • HTN

CS: cavernous sinus; ECA: external carotid artery; ICA: internal carotid artery; HTN: hypertension.

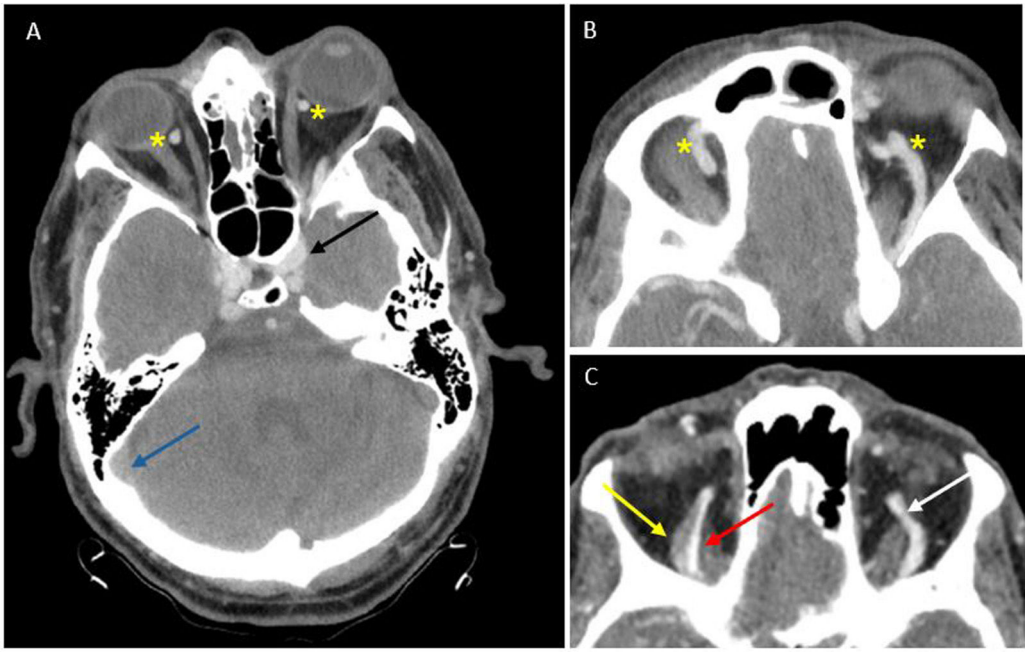


Figure 12 Vascular disease. (A and B) Carotid–cavernous fistula in a patient following head trauma. Axial sections from a cranial CT angiography in the arterial phase. Ectasia and hyperenhancement of the cavernous sinus (black arrow) are observed, with attenuation values similar to those of the internal carotid artery and higher than those of the other venous sinuses (sigmoid sinus, blue arrow). Dilatation of the superior ophthalmic veins (yellow asterisk), more marked on the left, and proptosis, also more evident on the left side. These findings were confirmed by cerebral angiography, followed by embolisation. (C) Partial thrombosis of the right superior ophthalmic vein. Cranial CT angiography in the venous phase in an 82-year-old man with cardiovascular risk factors and a history of sigmoid colon neoplasm, presenting to the emergency department with symptoms suggestive of left middle cerebral artery stroke, which was confirmed by imaging. Incidentally, dilatation of both ophthalmic veins was noted, with increased calibre of the right ophthalmic vein (yellow and red arrows) compared with the contralateral side (white arrow), showing partial opacification after intravenous contrast administration, consistent with partial thrombosis in its lateral aspect (yellow arrow).

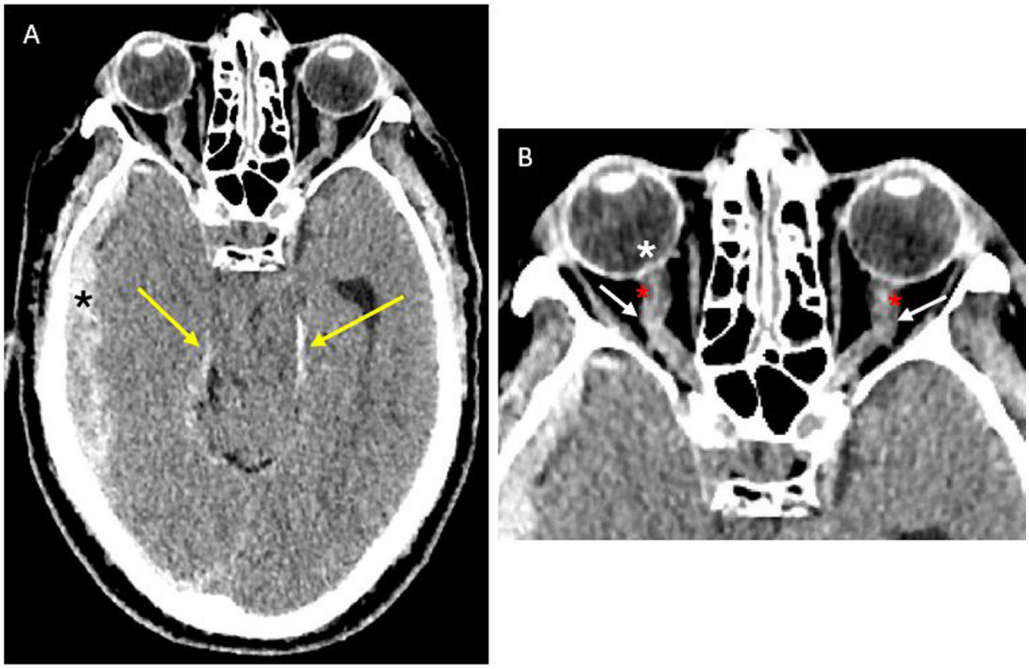


Figure 13 Bilateral papilloedema in a patient with head trauma. (A) Axial section from non-contrast cranial CT. Right convexity subdural haematoma (black asterisk) extending to the tentorium (yellow arrows), causing a degree of mass effect on the adjacent structures. Secondary bilateral papilloedema. (B) Detail of the orbits shown in image A. Note the bilateral thickening of the dural sheath of the optic nerves (red asterisks) and their tortuosity (white arrows). Flattening of the posterior aspect of the sclera is seen at the location of both optic discs, more marked on the right side (white asterisk).

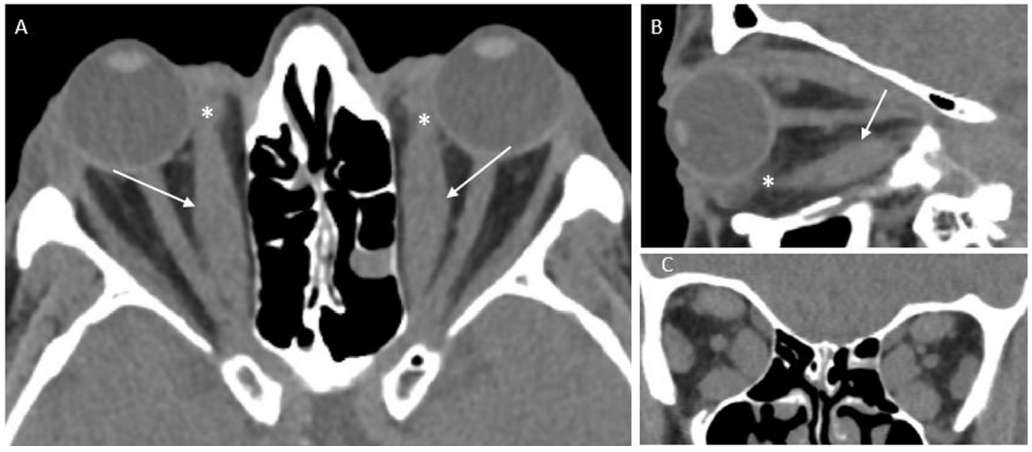


Figure 14 Thyroid eye disease. (A–C) Axial, sagittal and coronal planes of non-contrast orbital CT in a 50-year-old woman with bilateral exophthalmos and thickening of the extraocular muscle bellies (white arrows), with sparing of their tendinous insertions on the globe (asterisks). This thickening is most pronounced in the inferior and medial rectus muscles (image C).

of the lacrimal gland, eyelid oedema and reduced calibre of the optic nerve due to compression, which may lead to blindness.[1]

Orbital pseudotumour

Orbital pseudotumour involves a non-granulomatous inflammatory process of unknown aetiology.[1,2] The diagnosis is made by exclusion and with radiological findings include stranding of the orbital fat, thickening of one or more extraocular muscles with *involvement of the tendinous sheath*, an intraorbital mass (with enhancement following intravenous contrast administration), inflammation and enlargement of the lacrimal gland, and involvement of the optic nerve sheath, uvea and sclera. Corticosteroid therapy leads to rapid symptom improvement.[1,53,54] (Fig. 15)

Conclusions

Radiologists must be familiar with emergency ophthalmological conditions and understand the optimal CT protocol, taking into account the value of intravenous contrast admin-

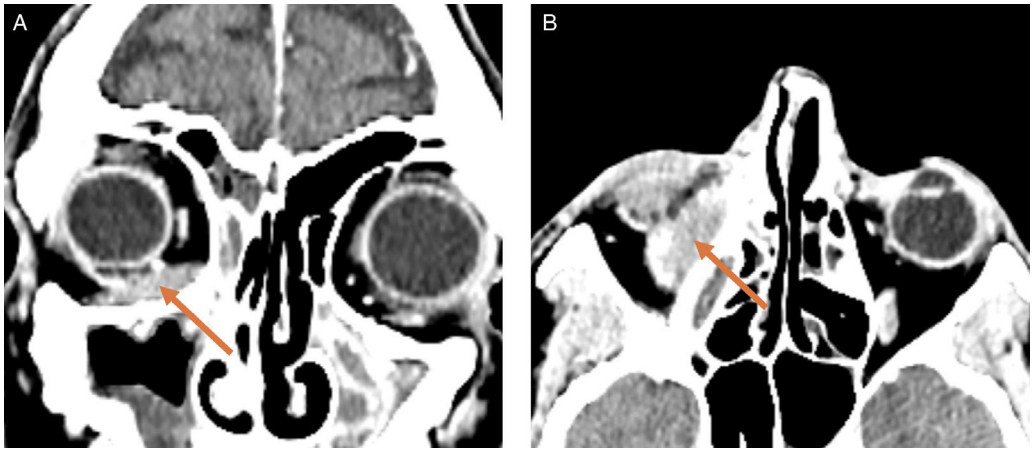


Figure 15 Right orbital pseudotumour (mass type). (A) Coronal reconstruction and (B) axial section of orbital CT after intravenous contrast administration, demonstrating an extraconal mass in inferior region of the right globe (orange arrows) with mild enhancement following contrast administration.

istration. Findings related to ocular infection, such as uveal thickening and hyperenhancement, can be subtle and difficult to identify. Differences in anterior chamber diameter, globe contour irregularities and the presence of intraocular foreign bodies are considered signs of globe rupture, which must be distinguished from potential mimics. Dilatation and early enhancement of the cavernous sinus, along with ectasia of the superior ophthalmic vein, pterygoid venous plexuses and the ipsilateral facial vein, are signs of a carotid–cavernous fistula. Symmetrical and bilateral thickening of the extraocular muscles with sparing of the tendinous insertion is a typical finding in thyroid eye disease, whereas involvement of the tendinous sheath suggests an orbital pseudotumour. Distinguishing between these two entities is important, as it alters the patient's therapeutic management.

CRediT authorship contribution statement

1 Research coordinators: MCMF, GSO, JEI.
2 Study concept: MCMF, GSO.
3 Study design: MCMF, GSO, LHVA, JEI.
4 Data collection: MCMF, GSO.
5 Data analysis and interpretation: all authors.
6 Data Processing: N/A.
7 Literature search: MCMF, GSO.
8 Drafting of article: MCMF, GSO, JEI.
9 Critical review of the manuscript with intellectually relevant contributions: all authors.
10 Approval of the final version: all authors.

Funding

This project has not received any funding.

Declaration of competing interest

The authors declare that there is no conflict of interest.

References

1. LeBedis CA, Sakai O. Nontraumatic orbital conditions: diagnosis with CT and MR imaging in the emergent setting. RadioGraphics. 2008;28(6):1741–53, http://dx.doi.org/10.1148/rg.286085515.
2. Nguyen VD, Singh AK, Altmeyer WB, Tantiwongkosi B. Demystifying orbital emergencies: a pictorial review. RadioGraphics. 2017;37(3):947–62, http://dx.doi.org/10.1148/rg.2017160119.
3. Ferreira TA, Saraiva P, Genders SW, Buchem MV, Luyten GPM, Beenakker J-W. CT and MR imaging of orbital inflammation. Neuroradiology. 2018;60:1253–66, http://dx.doi.org/10.1007/s00234-018-2103-4.
4. Thelen J, Bhatt AA, Bhatt AA. Emergency orbital pathology: what the radiologist should know. Emerg Radiol. 2017;24(5):585–92, http://dx.doi.org/10.1007/s10140-017-1528-0.
5. Sung EK, Nadgir RN, Fujita A, Siegel C, Ghafouri RH, Traband A, et al. Injuries of the globe: what can the radiologist offer? RadioGraphics. 2014;34(3):764–76, http://dx.doi.org/10.1148/rg.343135120.
6. Cellina M, Cè M, Marziali S, Irmici G, Gibelli D, Oliva G, et al. Computed tomography in traumatic orbital emergencies: a pictorial essay—imaging findings, tips, and report flowchart. Insights Imaging. 2022;13(4):1–17, http://dx.doi.org/10.1186/s13244-021-01142-y.
7. Mafee MF, Karimi A, Shah JD, Rapoport M, Ansari SA. Anatomy and pathology of the eye: role of MR imaging and CT. Magn Reson Imaging Clin N Am. 2006;14(2):249–70, http://dx.doi.org/10.1016/j.mric.2006.06.007.
8. Hallinan JTPD, Pillay P, Koh LHL, Goh KY, Yu W-Y. Eye globe abnormalities on MR and CT in adults: an anatomical approach. Korean J Radiol. 2016;17(5):664–73, http://dx.doi.org/10.3348/kjr.2016.17.5.664.
9. Radhakrishnan R, Cornelius R, Cunnane MB, Golnik K, Morales H. MR imaging findings of endophthalmitis. Neuroradiol J. 2016;29(2):122–9, http://dx.doi.org/10.1177/1971400916633480.
10. Malhotra A, Minja FJ, Crum A, Burrowes D. Ocular anatomy and cross-sectional imaging of the eye. Semin Ultrasound CT MRI. 2011;32(1):2–13, http://dx.doi.org/10.1053/j.sult.2010.10.009.

11. Smith AM, Czyz CN. Neuroanatomy, Cranial Nerve 2 (Optic). In: En: StatPearls [Internet]. Treasure Island (FL): StatPearls Publishing; 2022 [revisado 7 nov. 2022; acceso el 13 dic. 2023]. Available from: https://www.ncbi.nlm.nih.gov/books/NBK507907/
12. Sinnatamby Chummy S. Last's Anatomy. 12th ed Londres: Churchill Livingstone/Elsevier; 2018.
13. Lieber S, Fernandez-Miranda JC. Anatomy of the orbit. J Neurol Surg B Skull Base. 2020;81(4):319–32, http://dx.doi.org/10.1055/s-0040-1715096.
14. Shumway CL, Motlagh M, Wade M. Anatomy, Head and Neck, Eye Extraocular Muscles. In: En: StatPearls [Internet]. Treasure Island (FL): StatPearls Publishing; 2022 [revisado el 13 oct. de 2022; acceso el15dic.de2023]. Available from: https://www.ncbi.nlm.nih.gov/books/NBK519565/
15. Marqués E, Ferreiros N, Fernández LM, Sanz P, Castanedo D, Marco E, et al. Protocolos urgentes de Radiodiagnóstico. TC, RM e intervencionismo básico. 1st ed Torrelavega: Ediciones Valnera y Cenora; 2022.
16. American College of Radiology. ACR Appropriateness Criteria. Suspected orbital cellulitis, uveitis, or scleritis. Initial Imaging [revisado en 2017; acceso el 21 dic. de 2023]. Available from: https://gravitas.acr.org/ACPortal/GetDataForOneScenario?senarioId=3428.
17. American College of Radiology. ACR Appropriateness Criteria. Traumatic visual defect. Suspect orbital injury. Initial Imaging [revisado en 2017; acceso el 21 dic. de 2023]. Available from: https://acsearch.acr.org/docs/69486/Narrative/.
18. Jyani R, Ranade D, Joshi P. Spectrum of orbital cellulitis on magnetic resonance imaging. Cureus. 2020;12(8):e9663, http://dx.doi.org/10.7759/cureus.9663.
19. Platnick J, Crum AV, Soohoo S, Cedeño PA, Johnson MH. The globe: infection, inflammation, and systemic disease. Semin Ultrasound CT MRI. 2011;32(1):38–50, http://dx.doi.org/10.1053/j.sult.2010.12.003.
20. Pappuru R, Pravin V, Pathengay A, Gangakhedkar S, Sharma S, Nayayanan R, et al. Endophthalmitis progressing to panophthalmitis: clinical features, demographic profile, and factors predicting outcome. Semin Ophthalmol. 2018;33(5):671–4, http://dx.doi.org/10.1080/08820538.2017.1416411.
21. Connell PP, O'Neill EC, Fabinyi D, Islam FM, Buttery R, McCombe M, et al. Endogenous endophthalmitis: 10-year experience at a tertiary referral centre. Eye (Lond). 2011;25(1):66–72, http://dx.doi.org/10.1038/eye.2010.145.
22. Jackson TL, Eykyn SJ, Graham EM, Stanford MR. Endogenous bacterial endophthalmitis: a 17-year prospective series and review of 267 reported cases. Surv Ophthalmol. 2003;48(4):403–23, http://dx.doi.org/10.1016/s0039-6257(03)00054-7.
23. Sadiq MA, Hassan M, Agarwal A, Sarwar S, Toufeeq S, Soliman MK, et al. Endogenous endophthalmitis: diagnosis, management, and prognosis. J Ophthalmic Inflamm Infect. 2015;5(1):32, http://dx.doi.org/10.1186/s12348-015-0063-y.
24. Drancourt M, Whitby M. Endophthalmitis. In: Cohen J, Opal SM, Powderly WG, editors. Infectious Diseases. 3rd ed Mosby; 2010.
25. Ibañez L, Navallas M, de Cáceres IA, Martínez-Chamorro E, Borruel S. CT Features of posttramatic vision loss. AJR Am J Roentgenol. 2021;217(2):469–79, http://dx.doi.org/10.2214/AJR.20.24164.
26. Go JL, Vu VN, Lee KJ, Becker TS. Orbital trauma. Neuroimaging Clin N Am. 2002;12(2):311–24, http://dx.doi.org/10.1016/s1052-5149(02)00012-6.
27. Roy AA, Davagnanam I, Evanson J. Abnormalities of the globe. Clin Radiol. 2012;67(10):1011–22, http://dx.doi.org/10.1016/j.crad.2012.03.006.
28. Wang D, Rizzuti A. Eye trauma imaging. In: En: StatPearls [Internet]. Treasure Island (FL): StatPearls Publishing; 2023 [revisado el 26 jun. de 2023; acceso el 13 dic. de 2023]. Available from: https://www.ncbi.nlm.nih.gov/books/NBK572102/
29. Yoonessi R, Hussain A, Jang TB. Bedside ocular ultrasound for the detection of retinal detachment in the emergency department. Acad Emerg Med. 2010;17:913–7, http://dx.doi.org/10.1111/j.1553-2712.2010.00809.x.
30. Diep MQ, Madigan MC. Choroidal detachments: what do optometrists need to know? Clin Exp Optom. 2019;102(2):116–25, http://dx.doi.org/10.1111/cxo.12807.
31. Zhou Y, DiSclafani M, Jeang L, Shah AA. Open globe injuries: review of evaluation, management, and surgical pearls. Clin Ophthalmol. 2022;16:2545–59, http://dx.doi.org/10.2147/OPTH.S372011.
32. Kim SY, Lee JH, Lee YJ, Choi BS, Choi JW, In HS, et al. Diagnostic value of the anterior chamber depth of a globe on CT for detecting open-globe injury. Eur Radiol. 2010;20(5):1079–84, http://dx.doi.org/10.1007/s00330-009-1653-6.
33. Betts AM, O'Brien WT, Davies BW, Youssef OH. A systematic approach to CT evaluation of orbital trauma. Emerg Radiol. 2014;21:511–31, http://dx.doi.org/10.1007/s10140-014-1221-5.
34. Balakrishnan S, Harsini S, Reddy S, Tofighi S, Gholamrezanezhad A. Imaging reviewof ocular and optic nerve trauma. Emerg Radiol. 2020;27:75–85, http://dx.doi.org/10.1007/s10140-019-01730-y.
35. Gor DM, Kirsch CF, Leen J, Turbin R, Von Hagen S. Radiologic differentiation of intraocular glass: evaluation of imaging techniques, glass types, size, and effect of intraocular hemorrhage. AJR Am J Roentgenol. 2001;177(5):1199–203, http://dx.doi.org/10.2214/ajr.177.5.1771199.
36. Reiter MJ, Schwope RB, Kini JA, York GE, Suhr AW. Postoperative imaging of the orbital contents. RadioGraphics. 2015;35(1):221–34, http://dx.doi.org/10.1148/rg.351140008.
37. Lane JI, Watson RE, Witte RJ, McCannel CA. Retinal detachment: imaging of surgical treatments and complications. RadioGraphics. 2003;23(4):983–94, http://dx.doi.org/10.1148/rg.234025163.
38. Redmond-Craig A, Rajagopalan P, Lee J, Li J, Wong B, Zhang-Nunes S, et al. Imaging of the post-operative orbit and associated complications. J Clin Neurosci. 2021;89:437–47, http://dx.doi.org/10.1016/j.jocn.2021.05.031.
39. Pastor JC. GUIONES DE OFTALMOLOGÍA. Aprendizaje basado en competencias. 2nd ed Madrid: McGraw-Hills/Interamericana de España; 2012.
40. Adams A, Mankad K, Poitelea C, Verity DH, Davagnanam I. Post-operative orbital imaging: a focus on implants and prosthetic devices. Neuroradiology. 2014;56(11):925–35, http://dx.doi.org/10.1007/s00234-014-1403-6.
41. Kontos A, Tee J, Stuart A, Shalchi Z, Williamson TH. Duration of intraocular gases following vitreoretinal surgery. Graefes Arch Clin Exp Ophthalmol. 2017;255(2):231–6, http://dx.doi.org/10.1007/s00417-016-3438-3.
42. Patel A, Bhatt A, Kessler A. Radiology of abnormal globe contour. Clin Neuroradiol. 2021;31(1):1–9, http://dx.doi.org/10.1007/s00062-021-01049-7.
43. Kohli GS, Patel BC. Carotid Cavernous Fistula. In: En: StatPearls [Internet]. Treasure Island (FL): StatPearls Publishing; 2023 [revisado 3 abr. 2023; acceso el 13 dic. 2023]. Disponible en: https://www.ncbi.nlm.nih.gov/books/NBK535409/
44. Santos D, Monsignore LM, Nakiri GS, Cruz AAV, Colli BO, Abud DG. Imaging diagnosis of dural and direct cavernous carotid fistulae. Radiol Bras. 2014;47(4):251–5, http://dx.doi.org/10.1590/0100-3984.2013.1799.
45. Ringer AJ, Salud L, Tomsick TA. Carotid cavernous fistulas: anatomy, classification, and treatment. NeurosurgClinNAm. 2005;16(2):279–95, http://dx.doi.org/10.1016/j.nec.2004.08.004.

46. Lee JY, Jung C, Ihn YK, Kim DJ, Seong SO, Kwon BJ. Multidetector CT angiography in the diagnosis and classification of carotid-cavernous fistula. Clin Radiol. 2016;71(1):64–71, http://dx.doi.org/10.1016/j.crad.2015.10.018.
47. Sotoudeh H, Shafaat O, Aboueldahab N, Vaphiades M, Sotoudeh E, Bernstock J. Superior ophthalmic vein thrombosis: what radiologist and clinician must know? Eur J Radiol Open. 2019;11(6):258–64, http://dx.doi.org/10.1016/j.ejro.2019.07.002.
48. Rigi M, Almarzouqi S, Morgan M, Lee A. Papilledema: epidemiology, etiology, and clinical management. Eye Brain. 2015;7:47–57, http://dx.doi.org/10.2147/EB.S69174.
49. Watanabe A, Kinouchi H, Horikoshi T, Uchida M, Ishigame K. Effect of intracranial pressure on the diameter of the optic nerve sheath. J Neurosurg. 2018;109(2):255–8, http://dx.doi.org/10.3171/JNS/2008/109/8/0255.
50. Passi N, Degnan AJ, Levy LM. MR imaging of papilledema and visual pathways: effects of increased intracranial pressure and pathophysiologic mechanisms. AJNR Am J Neuroradiol. 2013;34(5):919–24, http://dx.doi.org/10.3174/ajnr.A3022.
51. Parmar H, Ibrahim M. Extrathyroidal manifestations of thyroid disease: thyroid ophthalmopathy. Neuroimaging Clin N Am. 2008;18(3):527–36, http://dx.doi.org/10.1016/j.nic.2008.03.003.
52. Müller-Forell W, Kahaly GJ. Neuroimaging of Graves' orbitopathy. Best Pract Res Clin Endocrinol Metab. 2012;26(3):259–71, http://dx.doi.org/10.1016/j.beem.2011.11.009.
53. Yuen SJ, Rubin PA. Idiopathic orbital inflammation: distribution, clinical features, and treatment outcome. Arch Ophthalmol. 2003;121(4):491–9, http://dx.doi.org/10.1001/archopht.121.4.491.
54. Pakdaman MN, Sepahdari AR, Elkhamary SM. Orbital inflammatory disease: pictorial review and differential diagnosis. World J Radiol. 2014;6(4):106–15, http://dx.doi.org/10.4329/wjr.v6.i4.106.